Holz als Roh- und Werkstoff 60 (2002) 96–105 © Springer-Verlag 2002
DOI 10.1007/s00107-002-0282-4

Investigations into the photodegradation of wood using microtensile testing

Part 4: Tensile properties and fractography of weathered wood

H. Turkulin, J. Sell

This paper describes an investigation into the relationship between the changes in tensile properties and structural integrity of wood during weathering. Investigated species were Scots pine (heartwood and sapwood, and separately earlywood and latewood), and Norway spruce. The photodegradation was monitored through the changes in microtensile strength of wood during natural and artificial UV-weathering ("thin strip" method), and by subsequent FE SEM microscopical analysis of transverse-fracture surfaces of the strips. The tensile strength changes during exposure (initial increase and two following phases of decrease) were analysed and were shown to be consistent with fractographic evidence of the structural changes in wood. These include the breakdown of compound middle lamella (CML), the thinning of cell walls and the development of brittleness of the secondary walls. The mechanism of failure is essentially different in earlywood and latewood, and the microtensile strength is predominantly determined by the latewood portions within growth rings.

Untersuchung des Photoabbaus von Holz mit Hilfe eines Mikro-Zugfestigkeitstests

Teil 4: Zug- und Brucheigenschaften von bewittertem Holz

Diese Arbeit beschreibt Untersuchungen der Beziehung zwischen den Änderungen der Zugfestigkeit und des Feingefüges von Holz infolge Wetterbeanspruchung. Untersucht wurden Kiefernholz (Kern- und Splintholz und, getrennt voneinander, Früh- und Spätholz) sowie Fichtenholz. Der Lichtabbau des Holzes wurde charakterisiert durch die Veränderung der Mikrozugfestigkeit während einer natürlichen und einer künstlichen UV- und Wetterbeanspruchung von dünnen (mikrotomierten) Holzstreifen ('thin strip'-Methode). Anschliessend wurden Querbruchflächen der Holzstreifen mit dem FE-SEM (Feldemissions-Rasterelektronenmikroskop) mikroskopisch analysiert. Die Änderung der Zugfestigkeit der Streifen während der Wetterexposition – anfänglicher Anstieg und nachfolgende Phasen des Rückgangs – wurden analysiert und erwiesen sich als übereinstimmend mit den fraktografischen Anzeichen der Gefügeveränderungen. Diese zeigten sich als Abbau der zusammengesetzten Mittellamelle, im Dünnerwerden und in einer Versprödung der Zellwände. Die Schädigungsmechanismen sind merklich unterschiedlich in Früh- und Spätholz. Die Mikrozugfestigkeit ist dominant vom Spätholzanteil der Jahrringe bestimmt.

1 Introduction

A series of investigations was performed to determine the influences of various factors, such as temperature, moisture, spectral light distribution and other physical aspects of exposures, on the weathering mechanisms and photodegradation rates in wood. The first two papers in this series (Derbyshire et al. 1995, 1996) demonstrated that the measurement of loss of microtensile strength of thin wood strips exposed to solar radiation offers a consistent and reliable means of determining photodegradation rates for wood. It was shown that artificial weathering regimes could provide good simulation of the effects of natural weathering and analytical procedures were developed to characterise the strength changes observed during weathering.

Part 3 (Derbyshire et al. 1997) described the application of the test methodology developed in Parts 1 and 2 to a study of the influence of temperature on photodegradation rates of a number of different softwood species during artificial weathering. The forthcoming paper shall report the results of an investigation into the influence of moisture on photodegradation rates. It was shown that moisture is detrimental for wood exposed to light and moisture proved a very influential accelerating factor in photo-induced degradation of wood (Turkulin 1996).

This fourth paper of a series presents the further analysis of mechanical aspects of monitoring the changes in wood during weathering by the consequences on microtensile strength, and the microscopic insight into the ultrastructural changes. Many former investigations of the weathering of wood also involved observations of the anatomical changes. Although microscopical observations are useful in providing information on the structural changes brought about by photodegradation, they cannot

H. Turkulin (✉)
Faculty of Forestry, University of Zagreb, Svetošimunska 25, 10000 Zagreb, Croatia

J. Sell
Swiss Federal Laboratories for Materials Testing and Research (EMPA), Ueberlandstr. 129, 8600 Dübendorf, Switzerland

The authors wish to express their gratitude to the EMPA, Building Research Est. UK and the Faculty of Forestry, for supporting this work which formed a part of the PhD thesis of the principal author. Thanks are also due to Dr Hilary Derbyshire and Dr E. Roy Miller, formerly with the BRE Ltd. UK, for helpful suggestions and comments.

quantify the degradation process. Furthermore, they give only general indications about the causes of the structural damage and can only detect changes in the more advanced stages of degradation. The main scope of this paper is to present the link between the highly accurate and reliable tensile strength measurements of thin strips and visual microscopic evidence of the structural deterioration caused by weathering.

2
Experimental

2.1
Preparation of thin strips

The following softwood species were used in the investigation: Scots pine sapwood (*Pinus sylvestris* L.) and Norway spruce (*Picea abies* Karst.).

The procedures for preparation and testing of the thin strips were fully reported earlier (Derbyshire et al. 1995, 1996); only brief details are given here. Blocks of dimensions 100 mm (L) × 10 mm (R) × 23–30 mm (T) were vacuum impregnated with distilled water at 20 °C until fully saturated. Strips of nominal thickness 70 μm or 80 μm were microtomed from the radial face of five blocks of each species using a sliding microtome. Radial strips were cut at some 5° to the real radial plane so that the rays do not stretch over the strip face. An additional set of tangentially cut strips was microtomed from the blocks matching those for radial sectioning; these sections were selected to be pure earlywood (70 μm) or latewood (50 μm) strips. After drying the strips in dark at 20 °C, 60%r.h., their mean thickness was determined from measurements on a representative sample from each block. Batches of 5 strips of each species were then selected for the determination of the tensile strength of the unweathered material at zero span and 10 mm span between the clamping jaws. These results, together with selected physical characteristics of the timbers, are detailed in Table 1.

2.2
Weathering of strips

For weathering the strips were mounted onto open aluminium frames, each designed to hold two test batches of five strips. The strips were fixed to the frames with double-sided adhesive tape, and for natural weathering they were backed with white filter paper and exposed horizontally at the BRE site (South-East England, 52°N, 70 m above sea level) between August and November 1993.

Artificial weathering was carried out using the QUV apparatus (Q-Panel Co) with fluorescent lamps of the 340 A type. The spectral output of the lamps was concentrated in the ultraviolet region of the spectrum between 290 and 400 nm, with peak intensity at 340 nm. The conditions in the QUV were maintained at 57 ± 2 °C, 95 ± 5% r.h.

The aluminium frames holding the samples without the backing aluminium panels were equipped with central dowels in the vertical axis; these fitted in the slots in the

Table 1. Wood characteristics and tensile strength data of wood species and strips tested
Tabelle 1. Merkmale und Zugfestigkeiten der geprüften Holzarten und Streifen

Species *Holzart*	Density *Rohdichte* kg/m^3 (at 20 °C, 60%rh)	No. of latewood bands per 10 mm width *Anzahl der Spätholzbänder per 10 mm*	Average Strip thickness *Mittlere Holz-streifen-dicke* (μm)	Tensile strength MPa (index to SPS radial strips) *Zugfestigkeit MPa (Index zu SPS Radialstreifen)*		
				Zero span	10 mm span	Index zero to 10 mm
Scots pine sapwood (SPS radial strips) *Kiefern-splintholz, Radial-streifen*	540	4–5	73	92 (1)	66 (1)	0.7
Scots pine Earlywood *Kiefern-frühholz*	(540)	–	68	83 (0.8)	60 (0.8)	0.7
Scots pine Latewood *Kiefern-spätholz*	(540)	–	50	318 (2.2)	264 (2.6)	0.83
Norway spruce *Fichte*	369	3–4	81.5	82	58	0.71

holder frames of the QUV. Thus no liquid water could have condensed on the strips. To compensate for the non-uniform distribution of intensity in the radiation output along the length of the lamps, a scheme for regular inversion of the frames and interchange of the sample positions was devised. This ensured that radiation doses for all samples were the same, and strips were irradiated on both faces by regular rotation of the frames around the dowels. Exposure of the strips continued until the strips were too fragile to test.

2.3 Tensile testing

Tensile tests were carried out on dry samples, after conditioning in dark at 20 ± 1 °C and 60 ± 5%r.h, using a Pulmac short span tensile tester. The ultimate breaking load of the strips was determined at zero and 10 mm span. In the zero span test, where the jaws are initially set in contact, all the microfibrils in the cross section bridge the gap between the jaws, and the test is basically a measure of microfibril, essentially cellulose, strength. The 10 mm span test measures matrix properties and the strength is to a greater extent determined by the strength of the lignin intercellular material and the degree of fiber bonding. Each value of ultimate breaking load was the mean of 10 replicate tests. Tensile strength values were expressed in terms of stress (in MPa) only for unweathered material (Table 1). In monitoring photodegradation, tensile strength changes were expressed as a percentage of the initial breaking load.

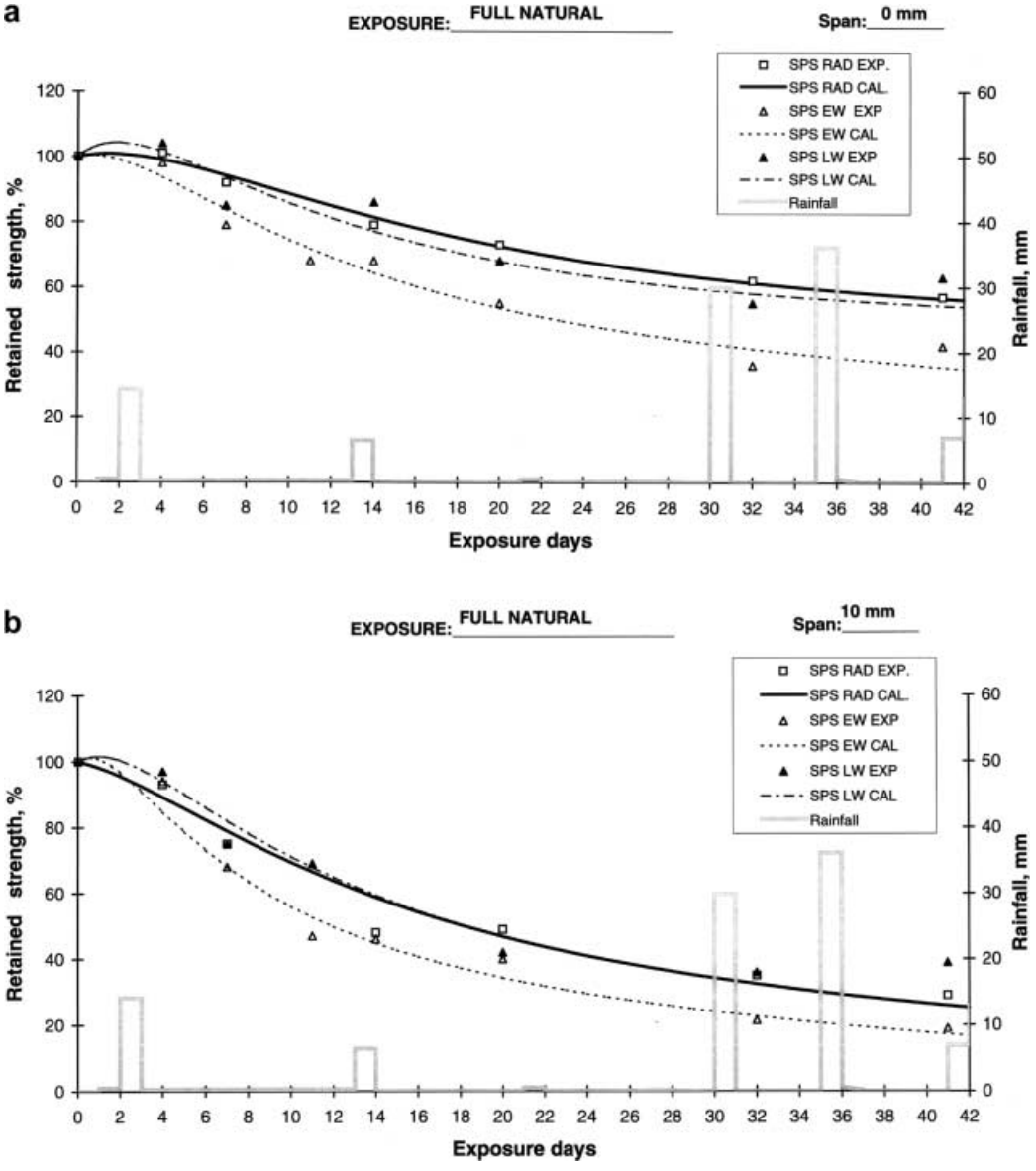

Fig. 1a, b. Strength changes of radial (RAD) strips, tangential earlywood (EW) and latewood (LW) strips of Scots pine sapwood and the rainfall during full natural exposure; *(a)* span 0 mm; *(b)* span 10 mm

Bild 1a, b. Prozentuale Rest-Längszugfestigkeit von dünnen radialen Kiefer-Streifen (RAD), und Streifen aus Frühholz (EW) und Spätholz (LW) in Abhängigkeit von der Dauer einer natürlichen Freibewitterung (die Balken geben die Niederschlagsmenge an). Messweite: *(a)* 0 mm; *(b)* 10 mm

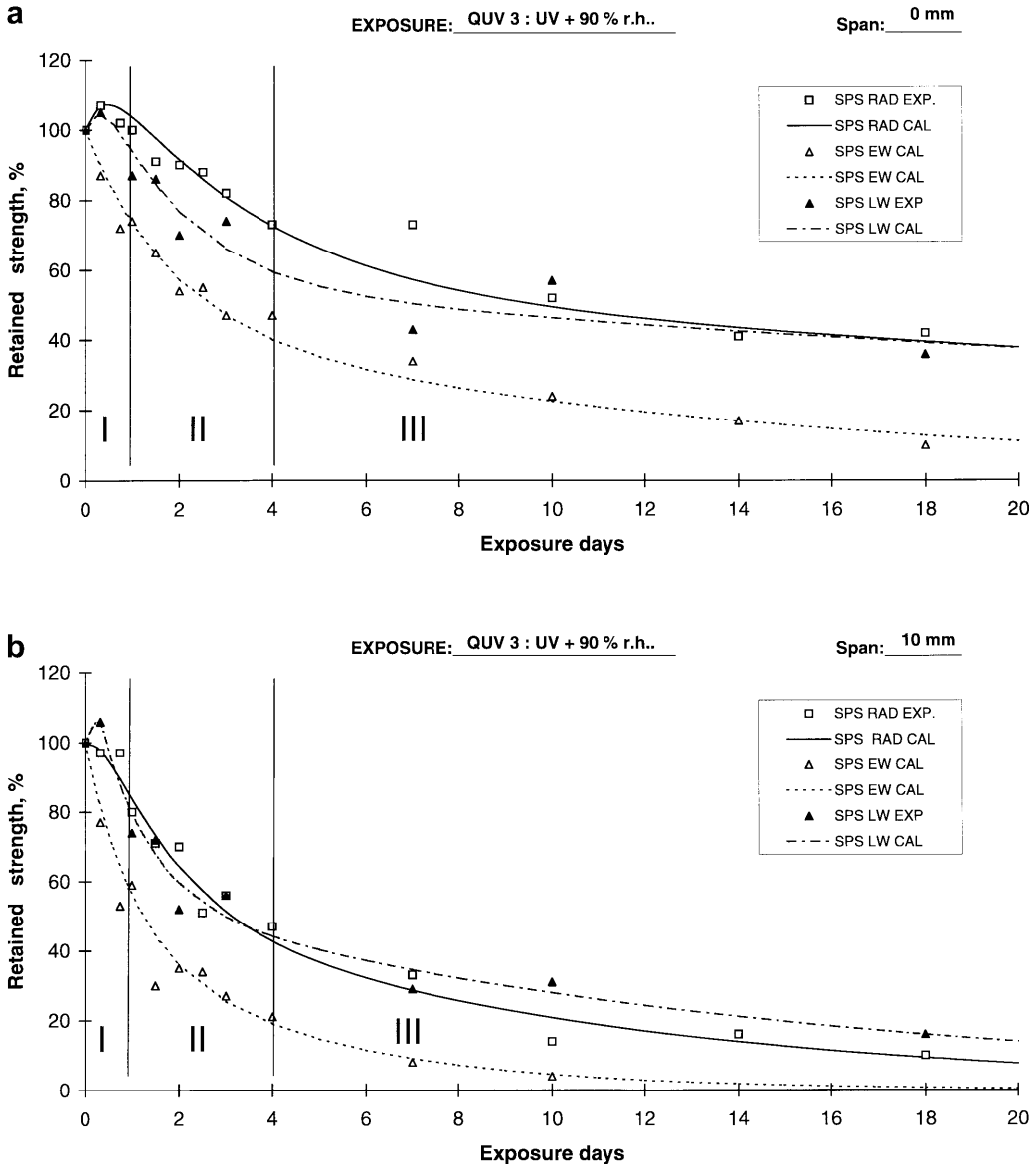

Fig. 2a, b. Strength changes of radial (RAD) strips, tangential earlywood (EW) and latewood (LW) strips of Scots pine sapwood during artificial exposure in humid (90% r.h.) conditions; (*a*) span 0 mm; (*b*) span 10 mm

Bild 2a, b. Prozentuale Rest-Längszugfestigkeit von dünnen radialen (RAD), tangentialen Frühholz (EW) und Spätholz (LW) Kiefernstreifen in Abhängigkeit von der Dauer einer künstlichen Bewitterung bei hoher Luftfeuchtigkeit (r.L. 90%). Messweite: (*a*) 0 mm; (*b*) 10 mm

2.4
Microscopic method

After tensile testing the remaining parts of the strips were stored for further examination into self-adhesive photo album sheets and some were later randomly chosen for SEM examination. In preparation for microscopic observation the strips were vacuum dried at 40 °C and sputtered with a layer of platinum, estimated to be ca. 15 nm thick (Zimmermann et al. 1994). The field-emission scanning electron microscope (FE-SEM) used was a JEOL JSM 6300 F situated at the EMPA. Micrographs were taken on ILFORD P4 PLUS film.

3
Results

3.1
Strength changes during weathering

Figures 1 and 2 present the losses in tensile strength for the exposure to different weathering cycles (note the different time-scales on the graphs).

The effect of exposure to high moisture conditions in artificial weathering (Figure 2) resulted in a degradation pattern which was closely similar, though more intensive and accelerated, than under natural exposure. For the

graphs shown in Figs. 1 and 2 the approximate time-acceleration factor was calculated to be 2.5.

The zero span strength tests on pine showed a period at the start of the natural exposure when the strength changed very little, and there was a 'shoulder' on the curve (Fig. 1). In humid conditions of UV exposure the strength actually increased at the initial period of the test (Fig. 2). This behaviour had been observed earlier in natural weathering trials (Derbyshire et al. 1995) and particularly with the pronounced effect of moisture (Turkulin 1996).

In order to compare the degradation rates for the different species in the various weathering cycles, the curves were analysed using the mathematical model developed in Part 2 (Derbyshire et al. 1996). The model was based on three simultaneously occurring radiation-induced processes. The first process, probably some form of radiation-induced cross-linking, resulted in a strength increase. The second and third processes represented the degradation of two components of the wood which degraded at different rates. The second phase would therefore be characterised predominantly by lignin degradation, and the final phase is dominated by the cellulose degradation rate. These postulations are discussed in detail and argumented in paper 2 of this series (Derbyshire et al. 1996). The method of analysis proved very accurate and could be adapted to

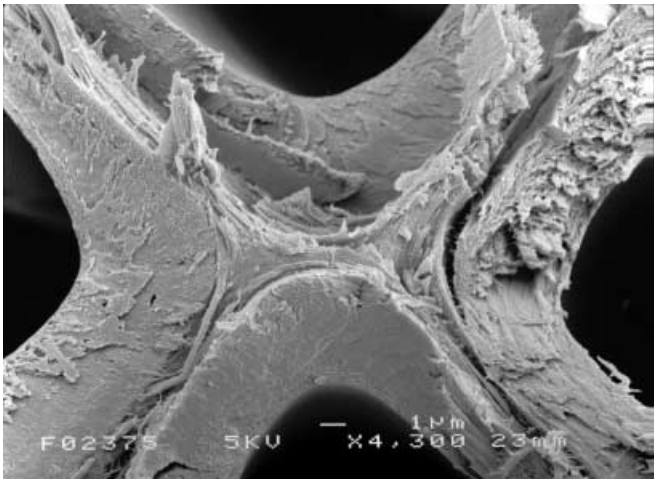

Fig. 3. Walls of pine latewood tracheids, unweathered (initial strength). Detail from Fig. 15. 4300:1
Bild 3. Zellwände von Spätholztracheiden von Kiefer, Detail (um 45° gedrecht) von Bild 15. 4300:1

Fig. 5. Walls of spruce earlywood tracheids at their corner joint, unweathered (initial strength). Tough, interlocked failure mode showing torn bundles and radial fibril agglomerations (structures of the S2 layer perpendicular to the middle lamella, arrows) 6500:1
Bild 5. Zellwände von vier Frühholztracheiden von Fichte im Eckbereich, unbewittert. Das Bruchbild zeigt herausgezogene Bündel und radiale Agglomerationen von Cellulosefibrillen (Anordnung in der dicken S2 – Schicht senkrecht zur Mittellamelle, (Pfeile), was für einen eher duktilen Bruch spricht. 6500:1

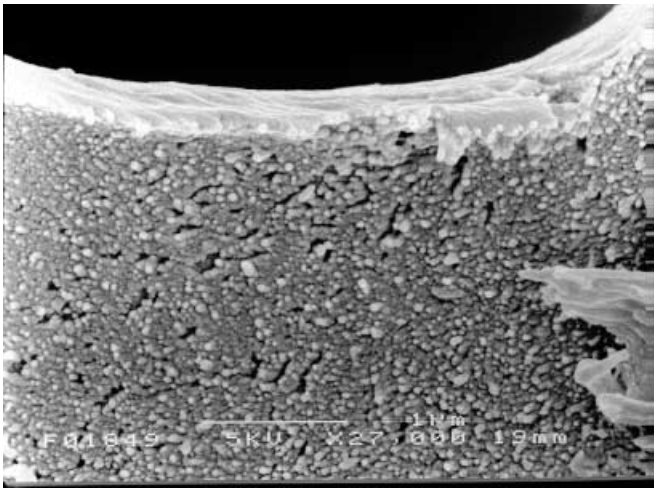

Fig. 4. Wall of a spruce latewood tracheid, unweathered, detail of the S2 and S3 layers. Brittle, smooth transverse fracture surface of the densely packed fibrils of the S2 layer. 27.000:1
Bild 4. Zellwand einer Spätholztracheide, unbewittert. Detail S3- und S2 – Schicht, wobei die ziemlich glatte Sprödbruchfläche auf den dicht gepackten Fibrillen der S2 – Schicht gut zu erkennen sind. 27000:1

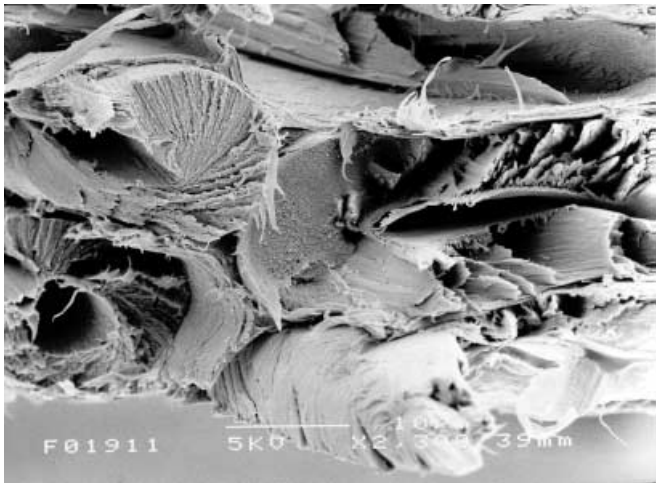

Fig. 6. Pine latewood tracheids, unweathered (initial strength), tested over zero span. Failure of the tough character revealing radial fibril agglomerations (arrows). 2300:1
Bild 6. Kiefernspätholztracheiden, unbewittert, Prüflänge null. Der eher verformungsreiche Bruch hat mehr oder weniger radiale Fibrillenagglomerationen der S2 sichtbar gemacht (Pfeile). 2300:1

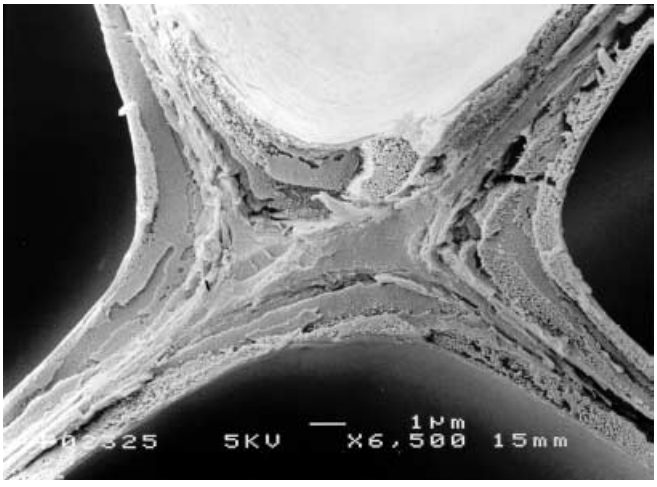

Fig. 7. Tracheid walls of Pine earlywood after QUV-3 (UV at high humidity) exposure for 72 h (10 mm span, 50% retained strength). Walls show brittle failure with delamination in the middle lamella region. 6500:1
Bild 7. Tracheidenwände von Kiefernfrühholz nach 72 Stunden Exposition im QUV – 3 Zyklus (UV- Belichtung bei hoher Luftfeuchte); 10 mm Prüflänge, 50% Restzugfestigkeit. Zellwände mit Sprödbruch und Delaminationen in der Mittellamelle. 6500:1

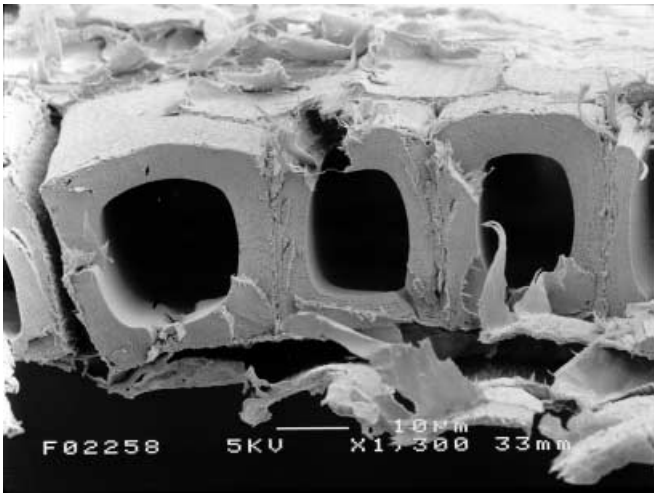

Fig. 8. Spruce latewood tracheids after natural exposure for 41 days (10 mm span, 40% retained strength). Thinned walls show brittle failure in a transverse plane. 1300:1
Bild 8. Tracheiden von Fichtenspätholz nach 41 Tagen Freibewitterung (10 mm Prüflänge, 40% Restzugfestigkeit). Die dünner gewordenen Zellwände zeigen glatte Sprödbrüche. 1300:1

describe the strength loss curves obtained from low humidity exposure to high humidity conditions, for natural weathering and various regimes of artificial exposures, and for various patterns of the tensile strength changes.

3.2
Micrographs

Microscopic photographs (Figs. 3, 4, 5, 6, 7, 8 and 9) present the cross-sectional fractured surfaces of thin strips. The microscopic analysis of the failure mode of tension-tested wood was shown to yield ample information about the physical condition of tested wood and fracture

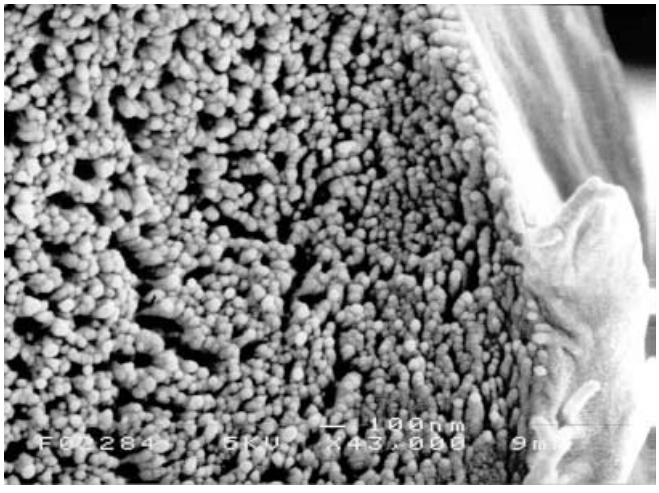

Fig. 9. Pine earlywood tracheid, S2/S3 layers, after natural exposure for 41 days (10 mm span, 40% retained strength). Blunt appearance of individual fibrils indicate cellulose degradation. Notice voids between fibrils and the absence of radial fibril agglomerations, presumably caused by the intense lignin degradation. 43000:1
Bild 9. S2/S3-Schicht einer Tracheidenwand von Kiefernfrühholz nach 41 Tagen Freibewitterung (10 mm Prüflänge, 40% Restzugfestigkeit). Stumpfe Bruchflächen der Fibrillen deuten auf einen Celluloseabbau. Beachte die Hohlräume zwischen den Fibrillen und das Fehlen radialer Fibrillenagglomerationen, vermutlich durch den weitgehenden Ligninabbau verursacht. 43000:1

progress (Derbyshire, Miller 1981, Zimmermann et al. 1994). The field-emission (FE SEM) microscope offered the advantages of high magnification at an accelerating voltage of 5 kV, low enough to avoid damage to the wood tissue. Low charging effect on the edges and points on the specimen enabled the fine structure of the fractured cells to be clearly visible. Failure characteristics are further explained in detailed figure captions and in chapter 4.3.

4
Discussion

4.1
Initial strength increase

The finding about the significant initial strength increase during UV irradiation is certainly the most exciting result of the research. The support to this observation can be found in the work by other authors (Kalnins and Knaebe 1992, Williams et al. 1990, Arnold et al. 1992), but was attributed to other factors.

The initial increase in strength, which dominates the strength changes in the first phase of UV irradiation at elevated humidity conditions, is now believed to be the consequence of (additional) cellulose crosslinking. This increase is short-lived and is usually associated with subsequent high rates of strength loss, so it does not reflect any long term increase in photo-resistance. Back (1967) claimed that the experimental evidence exists that UV-light can have an effect on the formation of carbonyl groups and subsequent crosslinking. Back himself experimentally obtained the thermal auto-crosslinking of cellulose (Back 1967, Didricksson and Back 1969) but at very high temperatures (above 200 °C). Horn et al. (1992)

during FT-IR studies on weathered wood also reported an increase in the intensity of the carbonyl band at 1750 cm^{-1} for short periods of weathering, followed by a decrease for longer exposure periods.

The fact that the increase observed in our research was always much greater in zero span testing than in 10 mm span testing links it with the cellulose properties, i.e. with the fibrilar tensile strength. It is not clear which type of reactions is involved, but it is speculated that it is either the increase in the state of order in the amorphous regions by forming small crystallites and by its partial inclusion in the crystalline regions which Hatakeyama et al. found to take place in the presence of water (Hatakayama et al. 1987). The other plausible theory is the increase in cellulose crystallinity (which naturally happens through the aggregation of cellulose chains into a microfibril simultaneously with its synthesis in a living tree) which may happen in the presence of water (Sarko 1987).

Desai and Shields (1970) were the first to postulate the possibility that the crosslinking in amorphous cellulose regions occurs during initial UV-irradiation of paper. It would be expected that covalent crosslinking should also result in the wet strength increase of paper. To the contrary, the shoulder was never recorded in wet testing of wood strips (Turkulin 1996).

Manwiller and Godfrey (1972) attributed the microtensile strengthening following the delignification to the mechanical effect of stress relaxation and more regular orientation of cellulosic structural elements. The strength increase was significantly greater in earlywood than in latewood, presumably due to differences in lignin content. In our tests, on the contrary, the zero span strength of earlywood never exhibited a pronounced increase in strength (Fig. 2).

Simple exposure to moisture or water, even without the effect of light, could cause instantaneous stress dissemination and strength increase. This was not reported by other authors (Evans and Banks 1988, 1990) and a gradual increase and decline of the shoulder (Fig. 2) seem to contradict this postulation. The nature of initial strength increase remains to be an issue of further research interest.

4.2
Earlywood/latewood tensile properties

To investigate the relative degradation rates of both ring portions and the effect of latewood strength in determination of photodegradation rates by tensile testing, the measurements have been conducted in parallel on the radial strips and tangential strips of pure latewood or earlywood. The results of the exposure of these specimens in full natural exposure and in artificial weathering trials are presented in Fig. 1 and 2. Additionally, Table 1 brings the numerical values of the initial ultimate tensile load.

It is obvious that the strength loss curves in both testing spans (0 and 10 mm) of radial strips during natural exposure (Fig. 1) and in the artificial weathering regime (Fig. 2) closely resemble those of the latewood strips. The rate of strength loss of radial strips is controlled by a change in latewood tensile properties.

Earlywood is more susceptible to photodegradation than latewood because of its greater light transparency, lower density, supposingly lower cell wall packing density (Wellwood et al. 1965), lower degree of cellulose polymerization (Ifju 1964) and up to 2% higher lignin content (Hon and Feist 1981). The application of tangential, pure earlywood strips in investigation of photostabilizing effects of various treatments can be advantageous in terms of shortening the exposures.

Tangentially cut material may have greater numbers of complete cells in strips due to the rectangular deformation of tracheids in tangential plane. Smaller numbers of obliquely cut and split cells in tangential strips may result in higher strength (see also Mark 1967, Biblis 1970). However, if ultimate load values for separate tangential strips were multiplied with the proportions of latewood/earlywood (e.g. 30%–70%) in the width of radial strips, then the strength values for these "proportional" strips woud not be the same as for real radial strips, but ca. 60–80% higher. This indicates that the failure mechanism of the wood structure is not the same in radial and tangential strips, which can actually withstand higher loads. Strength of latewood strips, multiplied with the approximate latewood proportion in the radial strips (0.30), matches very well with the actual strength of radial strips. This detail, along with the matching of the curves for radial and latewood strips (Fig. 2), strongly indicates that the strength and strength loss rate of radial strips mainly depend on the strength of their latewood portions. The postulation arises that the ultimate failure is initiated in the most stressed places in the latewood zone. Higher values of the "Index 10 mm to zero span" for latewood (Table 1) suggest that the extensibility of latewood is smaller than that of earlywood and this supports the postulation about the stress concentration in the latewood regions. However, the influence of earlywood portions on overall tensile properties cannot be neglected because of its role in transferring the stresses and enabling the dislocation of the stressed zones.

4.3
Discussion on fractographic findings

These wide ranging microscopic investigations encompassed both pine and spruce samples and also samples exposed to natural and artificial weathering. There were no notable effects that were specifically attributable to the species, the failure modes of pine and spruce were closely similar, especially when comparisons were made between the earlywood regions of the two species. Paajanen (1994) has also reported the lack of observable differences in the structural changes of pine and spruce after two years of natural weathering. It was also noticed that exposure to artificial weathering reproduced the changes in both failure mode and structural degradation brought about by natural weathering.

4.3.1
Fracture mode of unweathered strips

Finite span testing: In general, unweathered material tested in tension exhibits a type of failure characterized by an irregular surface in which the fracture of the cell wall leaves

bundles of microfibrils pulled out from each other. Examples of this "interlocked" failure for earlywood and latewood tracheids are presented in Figs. 3 and 5. Radial agglomerations of microfibrils and voids in the opposite fracture surfaces of the cell wall in the S2 layer can be seen (Fig. 5).

The appearance of the interlocked failure mode in earlywood regions is attributed to the greater extensibility of earlywood in comparison with latewood. Zimmermann et al. (1994) also noticed this effect, determined by the speed of failure. If the external load is applied slowly, plastic flow would result in the pulling out of strands and bundles of microfibrils (see Borgin 1971, Derbyshire and Miller 1981, Zimmermann et al. 1994). Sudden impact and a fast failure propagation results in brittle-like failure of the embedding matrix. It is not clear whether earlywood ribbons fail after latewood bands (as indicated here) or before. Bodner et al. (1997) showed that earlywood fails first, but they tested absolutely dry wood with very slow load increments, assuming the same extensibility of both ring poritons. We suppose that in thin strips the crack propagates very rapidly at the initiation of failure in the latewood zone leaving the fracture surfaces smooth (Figs. 3 and 4). As the critical stresses are released and the strain rapidly increases, failure develops in an irregular mode characterized by plastic flow and slippage between the fibrils (Fig. 5). This would support the theory that ultimate failure is initiated in the stiff latewood portions and that the tensile strength measurements obtained on radial strips are mainly determined by the latewood strength.

It is questioned whether anatomical discontinuities may constitute the points of weakness in thin strips. Bordered pits were not observed to influence the trans-wall fracture, although the crack sometimes follows their rims (Zimmermann 1994 see also Bodner et al. 1997 Harada 1965; Mark 1967 Cotè and Hanna 1983).

Debaise et al. (1966) postulated that longitudinal discontinuities can fail by distortion and delamination within the proportional stress-strain limits and thus contribute to the more uniformly distributed stress in axial tracheids. Some authors claimed that rays present the failure initiation points in compression testing (Delorme and Verhoff 1975, Keith and Cotè 1968), as well as in tension testing (Akande and Kyanka 1990, Côtè and Hanna 1983, and Zimmermann et al. 1994) although here the chronological order of events leading to ultimate failure was not clear. Bodner et al. (1997) indicated dual function of rays, both in transversal reinforcement and in longitudinal weakening of wood. Our investigation showed that the failure most often spread across the ray, only rarely following their direction. Rays incorporated in thicker strips (70–80 m) at a small angle to the surface (ca 5°), therefore, do not necessarily present the points of crack initiation.

Zero span testing: In zero span tests latewood fracture surfaces predominantly show a brittle appearance, and this failure mode only rarely develops into the interlocked mode (Fig. 6). It is more difficult to follow the path of the fracture initiation and crack progression here, because the elongation of the material prior to failure is much smaller than in finite span testing. Furthermore, damage by the jaws of the Pulmac tester can coincide with the line of failure.

The analysis leads to the conclusion that earlywood contributes very little to the tensile strength of thin strips. This supports the postulation in section 4.2. that the strength of radial strips is controlled by the strength of their latewood bands. The character of the failure in zero mm and in finite span tests is essentially the same, but greater influence of flaws and plastic deformations renders the strength values in 10 mm span testing lower.

4.3.2
The effect of weathering on fracture mode

There were three principal effects of weathering on the fracture mode of the thin strips. These were as follows: (1) contractions and delamination between cells and within cell wall layers, (2) thinning of the cell wall, and (3) development of brittleness.

Delamination. One notable effect of weathering (delignification in the second phase) was the detachment of the cells due to cohesive failure of the middle lamella, and this effect can be seen after only 4 days of natural weathering. It was notable that there were often large differences in the extent of delamination. The middle lamella sometimes retains a supprisingly large volume (Fig. 7, see also Bamber and Summerville 1981) but is sometimes almost completely disintegrated (Fig. 8).

Thinning of the cell walls. A reduction in thickness of the cell walls of earlywood was observed after moderate periods of exposure (compare Figs. 5 and 7). In latewood, a separation of the cells was observed; apparent thinning of the latewood cell walls was only observed after much longer periods of weathering (Fig. 8). These observations, which confirm earlier reports by Kuo and Hu (1991), suggest that lignin degradation may have resulted in a contraction of the cell wall volume.

Marked thinning of the cell walls is associated with a strength loss of 40–60%, which is coincident with the transition from the second to the third phase of the strength loss curve. That would mean that it is not the middle lamella decomposition, but the changes in the lignin structure in the S2 layer, which causes the steady reduction in strength and eventually results in the thinning of the cell walls. The high magnification of the S2 surface on Figure 9 show that the lignin degradation leaves microvoids between fibrils.

Brittleness. After moderate periods of exposure, there was a notable change in the mode of failure of earlywood cells from the interlocked failure, typical for unweathered wood, to brittle failure (compare Figs. 5 and 7). In the second weathering phase the fractured surfaces are smoothened which is a consequence of reduced flaw of the lignin-rich matrix on both cellular and ultrastructural level. Single fibrils show loss of radial agglomerations and mutual bonding. Latewood cells show a step-like progression of the crack and the failure develops to a lesser extent in an interlocked mode.

The third weathering phase induces almost perfectly brittle characteristics of the delignified surfaces (Fig. 9, compare it with Fig. 4). The crack generally propagates in a plane (Fig. 8), which suggests that there is very little elastic deformation prior to failure and that the progression of the crack is exceedingly rapid. Akande and Kyanka

(1990) noticed very similar structural changes caused by the action of *Gloeophyllum trabaeum*, a fungus which almost exclusively degrades cellulose. The similarity of their findings with the failure features in the third weathering phase confirms that the intensive cellulose degradation causes lesser resistance of the longitudinally oriented structural elements.

Whilst fractographic studies can contribute significantly to our understanding of the mechanisms of photodegradation it is important to realize their limitations. The examination of small sample areas may be unrepresentative, observations are frequently open to more than one interpretation and the results cannot give any quantitative measure of the degradation process. Notwithstanding these limitations, the FE SEM analysis has provided a valuable insight into the mechanisms of failure.

5 Conclusions

The mechanisms of tension failure in unweathered thin strips are basically different in earlywood and latewood. The mechanical properties of latewood dominate the tensile behaviour of radial strips. The findings indicate that the tension failure begins in latewood, where it develops in a brittle-like mode, and then spreads on earlywood zones in an interlocked, ductile mode.

The character of the tensile failure in zero and finite span tests is essentially the same. The lower values of 10 mm span strength are attributed to the greater influence of flaws and plastic deformations. The initial increase in strength during weathering cannot be substantiated by fractographic findings, and is believed to be a consequence of a cellulose crosslinking process.

During weathering the mode of failure progressively changes to brittle failure. Breakdown of the middle lamella during weathering has caused the detachment of surface cells – an effect observed early in the weathering process. Weathering also has caused the thinning of the cell walls – an effect interpreted as being caused by breakdown of the lignin in the S2 layer of the cell wall. This was thought to be the predominant process in the second phase of the strength loss during weathering. The development of brittle failure in earlywood was thought to be due to cellulose degradation in the final stages of weathering. The fractographic evidence was consistent with the three simultaneous weathering processes that explain the shape of the strength loss curves.

References

Akande JA, Kyanka GH (1990) Evaluation of tensile fracture in aspen using fractographic and theoretical methods. Wood Fiber Sci 22: 283–297

Arnold M, Feist WC, Williams RS (1992) Effect of weathering of new wood on the subsequent performance of semitransparent stains. For Prod J 42(3): 10–14

Arnold M, Sell J, Feist WC (1991) Wood weathering in fluorescent ultraviolet and xenon arc chambers. For Prod J 41: 40–44

Back EL (1967) Thermal auto-crosslinking in cellulose material. Pulp Paper Mag Can 66: T165–T171

Bamber RK, Summerville R (1981) Microscopic studies of the weathering of radiata pine sapwood. J Inst Wood Sci 9: 87–89

Biblis EJ (1970) Effect of thickness of microtome sections on their tensile properties. Wood Fiber Sci 2: 19–30

Bodner J, Schlag MG, Grüll G (1997) Fracture initiation and progress in wood specimens stressed in Tension. Part I.: Clear wood specimens stressed parallel to the grain. Holzforschung 51: 479–484

Borgin K (1971) The cohesive failure of wood studied with the scanning electron microscope. J. Microscopy 94(Pt 1) August 1971, 1–11

Côté WA, Hanna RB (1983) Ultrastructural characteristics of wood fracture surfaces. Wood Fiber 15: 135–163

Debaise GR, Porter AW, Pentoney RE (1966) Morphology and mechanics of wood fracture. Materials Research and Standards 6: 493–499

Delorme A, Verhoff S (1975) Zellwanddeformationen in sturmgeschädigtem Fichtenholz unter dem Rasterelektronenmikroskop. Holz Roh Werkstoff 33: 456–460

Derbyshire H, Miller ER (1981) The Photodegradation of wood during solar irradiation. Part 1. Effects on the structural integrity of thin wood strips. Holz Roh- Werkstoff 39: 341–350

Derbyshire H, Miller ER, Turkulin H (1995) Investigations into the photodegradation of wood using microtensile testing. Part 1: The application of microtensile testing to measurement of photodegradation rates. Holz Roh- Werkstoff 53: 339–345

Derbyshire H, Miller ER, Turkulin H (1996) Investigations into the photodegradation of wood using microtensile testing. Part 2: An investigation of the changes in tensile strength of different softwood species during natural weathering. Holz Roh- Werkstoff 54: 1–6

Derbyshire H, Miller ER, Turkulin H (1997) Investigations into the photodegradation of wood using microtensile testing. Part 3: The influence of temperature on photodegradation rates. Holz Roh- Werkstoff 55: 287–291

Desai RL, Shields JA (1970) Light-initiated crosslinking in cellulose. J. Polym. Sci., Polym. Let. 8: 839–842

Didricksson EIE, Back EL (1969) Four secondary transitions of cellulose material evaluated by ultrasonic pulse technique. Effects of auto-crosslinking and some additives on transitions characteristics. In: DH Page (ed): The physics and chemistry of wood pulp fibers. TAPPI STAP Series, No.8. New York: TAPPI, p. 217–227

Evans PD, Banks WB (1985) Degradation of wood surfaces by dilute acids. IRG document No IRG/WP/3326. The IRG Secretariat, Stockholm

Evans PD, Banks WB (1988) Degradation of wood surfaces by water. Changes in mechanical properties of thin wood strips. Holz Roh- Werkstoff 46: 427–435

Evans PD, Banks WB (1990) Degradation of wood surfaces by water. Weight losses and changes in ultrastructural and chemical composition. Holz Roh- Werkstoff 48: 159–163

Harada H (1965) Ultrastructure and organization of gymnosperm cell walls. In: Côté WA Jr (ed): Cellular Ultrastructure of Woody Plants. Syracuse, N.A. Syracuse University Press. pp 215–233

Hatakeyama T, Ikeda Y, Hatakeyama H (1987) Structural change of the amorphous region of cellulose in the presence of water. In: Kennedy JF, Phillips GO, Williams PA, Eds: Wood and cellulosics: industrial utilisation, biotechnology, structure and properties. Chichester: Ellis Horwood and John Wiley & Sons. Chapter 2: 23–31

Hon DN-S, Feist WC (1981) Free radical formation in wood: the role of water. Wood Sci 14: 41–48

Horn BA, Qiu J, Owen NL, Feist WC (1992) FT-IR studies of weathering effects in Western red cedar and Southern pine. In: Chemical modification of lignocellulosics. FRI Bull 176. 1992 November 7–8, Rotorua, New Zealand: 67–76. Forest Research Institute, Rotorua, New Zealand

Ifju G (1964) Tensile strength behavior as a function of cellulose in wood. For Prod J 21: 366–372

Kalnins MA, Knaebe MT (1992) Wettability of weathered wood. J Adhesion Sci Tech 6: 1325–1330
Keith CT, Côté WA Jr (1968) Microscopic characterization of slip lines and compression failures in wood cell walls. For Prod J 18: 67–74
Kellog RM (1989) Density and porosity (of wood). In: Concise encyclopedia of wood and wood-based materials. Ed. A.P. Schniewind. Pergamon Press, Oxford:79–82
Kollmann FP, Côté WA. (1968) Principles of wood science and technology. Vol. 1. Solid wood. New York: Springer
Kuo M-L, Hu N (1991) Ultrastructural changes of photodegradation of wood surfaces exposed to UV. Holzforschung 45: 347–353
Manwiller FG, Godfrey PR (1972) Microtensile strength of spruce pine after exposure to acids and bases. Wood Sci 5: 295–297
Mark RE (1967) Cell wall mechanics of tracheids. New Haven and London: Yale University Press
Paajanen L (1994) Structural changes in primed Scots pine and Norway spruce during weathering. Materials and Structures 27: 237–244
Sarko A (1987) Cellulose – how much do we know about ist structure? In: Kennedy JF, Phillips GO, Williams PA (Eds. 1990): Wood and cellulosics: industrial utilisation, biotechnology, structure and properties. Chichester: Ellis Horwood and John Wiley & Sons. Chapter 6: 55–71
Timell TE (1989) Chemical composition (of wood). In: Concise encyclopedia of wood and wood-based materials. Ed. AP Schniewind. Pergamon Press, Oxford: 47–53
Turkulin H (1996) Photodegradation of exterior timber building components. Dissertation. Faculty of Forestry, Zagreb University. Zagreb, Croatia: 285 pp.
Wellwood RW, Ifju G, Wilson JW (1965) Intra-increment physical properties of certain western Canadian coniferous species. In: Côtè, W.A. Jr. (ed): Cellular Ultrastructure of Woody Plants. Syracuse, NY. Syracuse University Press. pp 539–549
Zimmermann T, Sell J, Eckstein D (1994) Rasterelektronenmikroskopische Untersuchungen an Zugbruchflächen von Fichtenholz. Holz Roh Werkstoff 53: 223–229